

Anti-GZK effect in Ultra High Energy Cosmic Rays diffusive propagation

R. Aloisio and V.S. Berezinsky

INFN - Laboratori Nazionali del Gran Sasso, I-67010 Assergi (AQ), Italy

ABSTRACT

We discuss the antiGZK effect in the diffusive propagation of ultra high energy protons in intergalactic magnetic fields, which consists in a jump-like increase of the maximum distance from which ultra high energy protons can reach an observer. The position of this jump, $E_j \approx 2 \times 10^{18}$ eV, is determined exclusively by energy losses (transition from adiabatic to pair-production energy losses) and it is independent of the diffusion parameters. The diffuse spectrum presents a low-energy steepening approximately at this energy, which is very close to the position of the second knee observed in the cosmic ray spectrum. The dip, seen in the universal spectrum as a signature of the interaction with the cosmic microwave background radiation, is also present in the case of diffusive propagation in magnetic fields.

Subject headings: UHE Cosmic rays, diffusive propagation, GZK cutoff.

1. Introduction

The GZK cutoff (Greisen (1966), Zatsepin and Kuzmin (1966)) is a steepening of the ultra high energy (UHE) protons spectrum due to the interaction with the cosmic microwave background (CMB) radiation. The presence of an intergalactic magnetic field can modify the GZK cutoff up to its absence in the case of very strong magnetic fields, Sigl et al (2004), Yoshiguchi et al (2003), (for a physical explanation of this effect see Aloisio and Berezinsky (2004)). The proton propagation in magnetic field can affect the observed UHE proton spectrum also at energies (much) lower than the GZK cutoff. The crucial parameter which determines the modification of the spectrum is the distance d between sources. If this distance is much less than all propagation distances, such as energy-attenuation length, l_{att} , and diffusion length l_{diff} , the spectrum is not distorted and has a universal (standard) shape (Aloisio and Berezinsky (2004)). This statement has the status of a theorem.

All these effects depend strongly on the strength of the large-scale intergalactic magnetic field (IMF), the knowledge of which still remains poor. The modes of the UHE-proton propagation vary between quasi-rectilinear propagation in a weak field and diffusive propagation in a strong magnetic field. The experimental data on IMF and the models of origin of these fields do not allow at present to choose even between the two extreme propagation regimes mentioned above.

The most reliable observations of the intergalactic magnetic field are based on the Faraday rotation of the polarized radio emission (for reviews see Kronberg (1994), Vallé (1997), Carilli and Taylor (2002)). The upper limit on the Faraday rotation measure (RM) in the extragalactic magnetic field, obtained from the observations of distant quasars, gives $RM < 5 \text{ rad/m}^2$. It implies an upper limit on the extragalactic magnetic field on each assumed scale of coherence length (Kronberg (1994), Vallé (1997), Ryu et al. (1998)). For example, according to Blasi et al. (1999a), for an inhomogeneous universe $B_{l_c} < 4 \text{ nG}$ on a scale of coherence $l_c = 50 \text{ Mpc}$.

According to observations of the Faraday rotations the extragalactic magnetic field is strongest, or order of $1 \mu\text{G}$, in clusters of galaxies and radiolobes of radiogalaxies (Vallé (1997), Kronberg (1994), Carilli and Taylor (2002)). The largest scale in both structures reaches $l_c \sim 1 \text{ Mpc}$. Most probably various structures of the universe differ dramatically by magnetic fields, with very weak field in voids and much stronger in the filaments (Ryu et al. (1998)). Superclusters seem to be too young for the regular magnetic field to be formed in these structures on a large scale $l_c \sim 10 \text{ Mpc}$.

In the case of a hierarchical magnetic field structures in the universe, UHE protons with $E > 4 \times 10^{19} \text{ eV}$ can propagate in a quasi-rectilinear regime. Scattering of UHE protons occurs mostly in galaxy clusters, radiolobes and filaments. Deflections of UHE protons can be large for some directions and small for the others. The universe looks like a leaky, worm-holed box, and correlation with the sources can be observable (see Tinyakov and Tkachev (2001), where correlations of ultra high energy cosmic rays (UHECR) with BLLacs are found). Such a picture has been suggested by Berezinsky et al. (2002b).

A promising theoretical tool to predict the IMF in large scale structures is given by magneto-hydrodynamic (MHD) simulations. The main uncertainty in these simulations is related to the assumptions concerning the seed magnetic field.

The MHD simulations of Sigl et al. (2004) and Sigl et al. (2003) favor a hierarchical structure with strong magnetic fields. Assuming an inhomogeneous seed magnetic field generated by cosmic shocks through the Biermann battery mechanism, the authors obtain $\sim 100 \text{ nG}$ magnetic field in filaments and $\sim 1 \text{ nG}$ in voids. In some cases they consider IMF

up to a few micro Gauss as allowed. In these simulations UHECR are characterized by large deflection angles, of the order of 20° , at energies up to $E \sim 10^{20}$ eV (Sigl et al. (2003), Sigl et al. (2004)). Thus, the scenario that emerges in these simulations seems to exclude the possibility of an UHECR astronomy. These simulations have some ambiguity related to the choice of magnetic field at the position of the observer (Sigl et al. (2003), Sigl et al. (2004)). The authors consider two cases: a strong local magnetic field $B \sim 100$ nG and a weak field $B \ll 100$ nG. The different assumptions about the local magnetic field strongly affects the conclusions about UHECR spectrum and anisotropy.

The essential step forward in MHD simulations has been made by Dolag et al. (2003). In this work the Local Universe is simulated with the observed density and velocity field. This eliminates the ambiguity for the local magnetic field, that is found to be weak. The seed magnetic field, used in this simulation, is normalized by the observed magnetic field in rich clusters of galaxies. The results of these constrained simulations indicate a weak magnetic fields in the universe of the order of 0.1 nG in typical filaments and of 0.01 nG in voids. The strong large-scale magnetic field, $B \sim 10^3$ nG, exists in clusters of galaxies, which, however, occupy insignificant volume of the universe. The picture that emerges from the simulations of Dolag et al. (2003) favors a hierarchical magnetic field structure characterized by weak magnetic fields. UHE protons with $E > 4 \times 10^{19}$ eV can propagate in a quasi-rectilinear regime, with the expected deflection angles being very small $\leq 1^\circ$.

The case of strong magnetic fields up to $1 \mu\text{G}$ has been studied in Sigl et al. (1999), Lemoine et al. (1999), Stanev (2000), Harari et al. (2002), Yoshiguchi et al. (2003), Deligny et al. (2003). The interesting features found in these calculations are small-scale clustering of UHE particles as observed by Hayashida et al. (1996), Hayashida et al. (1999), Uchiori et al. (2000), Glushkov and Pravdin (2001), and absence of the GZK cutoff in the diffusive propagation, when the magnetic field is very strong. Many aspects of the diffusion of UHECR have been studied in numerical simulation by Casse et al. (2002).

The small-scale clustering allows to estimate the space density of the sources (Dubovsky et al (2000) and Fodor and Katz (2000)). The recent Monte Carlo simulations (Yoshiguchi et al (2003), Blasi and De Marco (2004) and Kachelrieß and Semikoz (2004)) favor a number density of the sources $n_s \sim (1 - 3) \times 10^{-5} \text{ Mpc}^{-3}$ with rather large uncertainties (Blasi and De Marco (2004)).

Diffusive propagation of extragalactic UHECR has been studied already in earlier work. The stationary diffusion from Virgo cluster was considered by Wdowczyk and Wolfendale (1979), Giller et al. (1980) and non-stationary diffusion from a nearby source was studied by Berezinsky et al. (1990a), Blasi and Olinto (1999b) using the Syrovatsky solution (Syrovatskii (1959)) of the diffusion equation. In this case the GZK cutoff may be absent.

A very interesting phenomenon, caused by propagation of UHE protons in the extra-galactic magnetic fields, has been recently found by Lemoine (2004). It consists in a low-energy steepening of the spectrum of UHE protons at energies below 1×10^{18} eV produced by a large diffusive propagation time (exceeding the age of the universe) to the nearby sources. In this paper, we shall discuss the anti-GZK effect in diffusive propagation of UHE protons which is responsible for this low-energy steepening and discuss the transition from galactic to extragalactic cosmic rays. In our calculations we shall follow, like Lemoine (2004), the theoretical approach of Aloisio and Berezinsky (2004).

2. Diffusive propagation in the analytic approach

The analysis below is based on the analytical solution of the diffusion equation, found by Syrovatskii (1959). Using a distribution of sources on a lattice, the diffuse flux can be calculated as the sum over the fluxes from the discrete sources i :

$$J_p^{diff}(E) = \frac{c}{4\pi} \frac{L_p K(\gamma_g)}{b(E)} \sum_i \int_E^{E_g^{\max}} dE_g q_{gen}(E_g) \frac{\exp\left[-\frac{r_i^2}{4\lambda(E, E_g)}\right]}{(4\pi\lambda(E, E_g))^{3/2}}, \quad (1)$$

where $b(E) = dE/dt$ is the proton energy loss, summation goes over all lattice vertexes, L_p is the proton luminosity of a source, $q(E_g) = E^{-\gamma_g}$ is the generation function, and $K(\gamma_g)$ is the normalization coefficient equal to $\gamma_g - 2$ if $\gamma_g > 2$ and $1/\ln(E_{\max}/E_{\min})$, if $\gamma_g = 2$ (all energies are measured in GeV), and

$$\lambda(E, E_g) = \int_E^{E_g} d\epsilon \frac{D(\epsilon)}{b(\epsilon)} \quad (2)$$

is the Syrovatsky variable, which has the physical meaning of the squared distance traversed by a proton in the observer direction, while its energy diminishes from E_g to E . From Eq. (1) one can see that the sources at distances $r > 2\sqrt{\lambda(E, E_g)}$ give negligible contribution to the flux.

In our calculations we shall use also the second Syrovatsky variable, which can be understood as the time needed by a proton to diminish its energy from E_g to E :

$$\tau(E, E_g) = \int_E^{E_g} \frac{d\epsilon}{b(\epsilon)} . \quad (3)$$

The Syrovatsky solution formally includes all propagation times up to $t \rightarrow \infty$ and the generation energies are restricted from above only by the maximum acceleration energy E_{\max}^{acc}

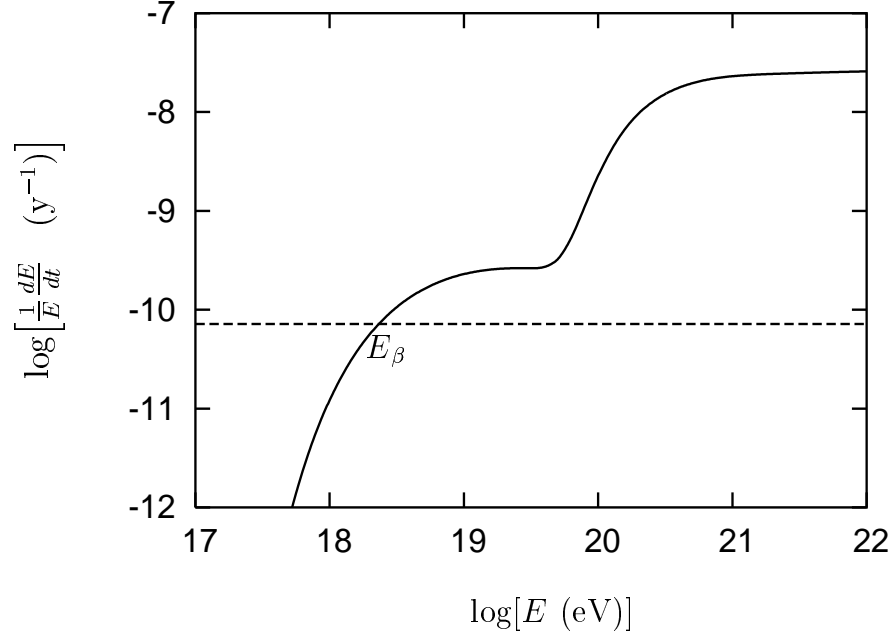


Fig. 1.— Proton energy losses. The continuous line represents the sum of pair production and photopion production energy losses, while the dashed line gives adiabatic energy losses $(1/E)(dE/dt) = H_0$. The label E_β shows the energy where pair-production and adiabatic energy losses are equal.

that a source can provide. In our case the propagation time from a source at fixed distance r must be smaller than the age of the universe t_0 , and due to this condition one more upper limit on the maximum generation energy E_g^{\max} emerges. This limit is given by the condition $\tau(E, E_g) \leq t_0$ and results in $E_g^{\max}(E) \leq E_g(E, t_0)$, which can be calculated also by evolving energy backward in time from E at $t = 0$ to E_g at $t = t_0$.

The upper limit E_g^{\max} in Eq. (1) is then the minimum between the two quantities: $E_g(E, t_0)$ and the maximal acceleration energy E_{\max}^{acc} ,

$$E_g^{\max}(E) = \min[E_g(E, t_0), E_{\max}^{\text{acc}}]. \quad (4)$$

At small energies $E \leq 2 \times 10^{18}$ eV $E_g(E, t_0) < E_{\max}^{\text{acc}}$, while at larger energies $E_g(E, t_0) > E_{\max}^{\text{acc}}$. In the calculations below we will assume $E_{\max}^{\text{acc}} = 1 \times 10^{22}$ eV.

The crucial quantity in the following discussion, the proton energy loss $\beta(E) = (1/E)dE/dt$, is shown in Fig. 1. Note the characteristic energy $E_\beta \approx 2 \times 10^{18}$ eV, where the pair-production energy losses $\beta_{e^+e^-}(E)$ reach the adiabatic energy losses.

Using these energy losses we can calculate $E_g^{\max}(E)$. The results are presented in Fig.

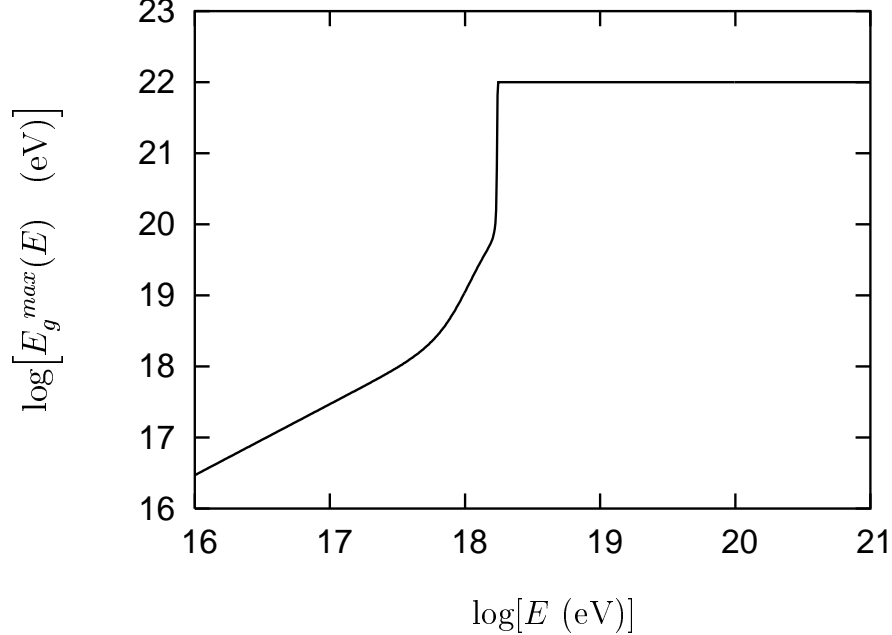


Fig. 2.— Maximum generation energy E_g^{\max} defined as $\min[E_g(E, t_0), E_{\max}^{\text{acc}}]$, where E_{\max}^{acc} is the maximal acceleration energy and t_0 is the age of the universe (see text).

2. At low energies $E_g(E, t_0)$ increases due to adiabatic energy losses. At the end of this stage the increase becomes more sharp because at large time t the pair-production energy-losses set in. Finally at $E \sim E_\beta$ $E_g(E, t_0)$ abruptly increases up to E_{\max}^{acc} practically by a jump. The jump factor is roughly given by $\exp(t_0/\bar{\tau})$, where $\bar{\tau}$ is the energy-loss time which diminishes as the energy rises with the backward time. This behavior of $E_g^{\max}(E)$ is responsible for the antiGZK effect, which will be discussed in the next Section.

We shall specify now the diffusion coefficient $D(E)$, which determines $\lambda(E, E_g)$ in Eq. (2). In the following discussion we shall also use the diffusion length definition as: $l_d(E) = 3D(E)/c$.

We assume diffusion in a random magnetic field with a strength B_0 on the maximum coherent length l_c , denoting this magnetic configuration by (B_0, l_c) . This assumption determines the diffusion coefficient $D(E)$ at the highest energies when the proton Larmor radius, $r_L(E) \gg l_c$:

$$D(E) = \frac{1}{3} \frac{cr_L^2(E)}{l_c} \quad (5)$$

At “low” energies, when $r_L(E) \lesssim l_c$ we shall consider three cases:

(i) The Kolmogorov diffusion coefficient

$$D_K(E) = \frac{1}{3} cl_c \left(\frac{r_L(E)}{l_c} \right)^{1/3}, \quad (6)$$

(ii) The Bohm diffusion coefficient

$$D_B(E) = \frac{1}{3} cr_L(E), \quad (7)$$

(iii) An arbitrary case $D(E) \propto E^\alpha$, with $\alpha = 2$ for the extreme energy regime.

In all cases we normalize the diffusion coefficient by $(1/3)cl_c$ at $r_L = l_c$. The characteristic energy E_c of the transition between the high energy and low energy regimes is determined by the condition $r_L(E) = l_c$ and is

$$E_c = 0.93 \times 10^{18} \left(\frac{B_0}{1 \text{ nG}} \right) \left(\frac{l_c}{\text{Mpc}} \right) \text{ eV.} \quad (8)$$

The smooth transition between the low-energy and high-energy diffusion regimes is provided with the help of an interpolation formula for the diffusion length:

$$l_{\text{diff}}(E) = \Lambda_d + \frac{r_L^2(E)}{l_c} \quad (9)$$

with $\Lambda_d = r_L(E)$ for the Bohm diffusion and $\Lambda_d = l_c(r_L/l_c)^{1/3}$ for the Kolmogorov regime.

For completeness we shall give also the numerical expression for the Larmor radius:

$$r_L(E) = 1.08 \times 10^2 \frac{E}{1 \times 10^{20} \text{ eV}} \frac{1 \text{ nG}}{B} \text{ Mpc.} \quad (10)$$

At distances $r \leq l_{\text{diff}}(E)$, the fluxes from individual sources i are calculated in the rectilinear approximation, and the diffuse flux is given by

$$J_p^{\text{rect}}(E) = \frac{L_p K(\gamma_g)}{(4\pi)^2} \sum_i \frac{q_{\text{gen}}(E_g(E, r_i))}{r_i^2} \frac{dE_g(E, r)}{dE} \quad (11)$$

where dE_g/dE is given in Berezinsky et al. (2002a).

3. Anti-GZK cutoff

In this Section we shall demonstrate that, in contrast to the GZK cutoff, increasing of the proton energy losses at energy $E \geq 1 \times 10^{18}$ eV results, in the case of diffusive propagation, in an *increase* of the maximal distance from which protons can arrive.

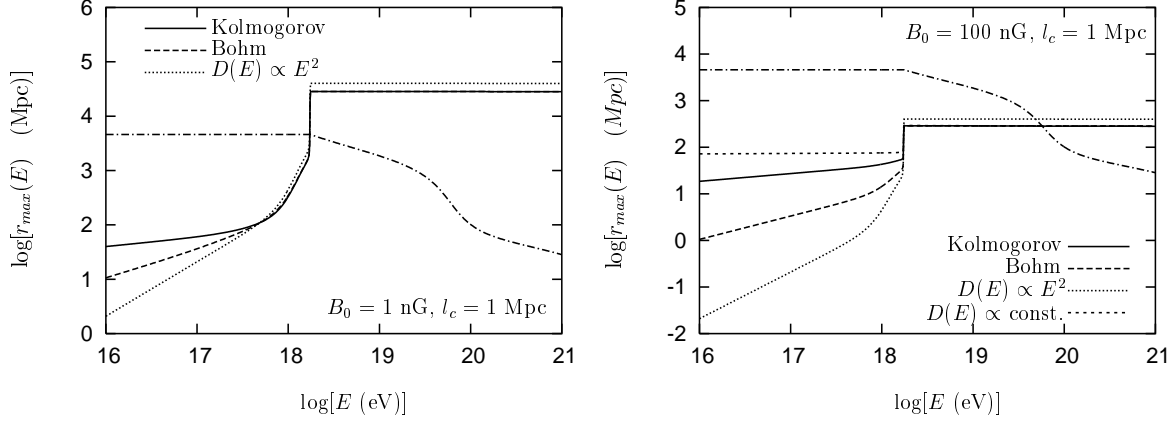


Fig. 3.— Maximal distance $r_{\max}(E)$ to the contributing sources as function of the observed energy E . Three merging curves in the left-low corner give $r_{\max}^{\text{diff}}(E)$ and the dash-dotted curve gives $r_{\max}^{\text{rect}}(E)$, which numerically is very close to the energy-attenuation length $l_{\text{att}}(E) = [(1/cE)dE/dt]^{-1}$. Continuous line is for the Kolmogorov diffusion $D(E) \propto E^{1/3}$ at $E \leq E_c$, dashed line - the Bohm diffusion $D(E) \propto E$, and dotted line - the extreme high-energy diffusion $D(E) \propto E^2$. In the right panel $D(E) = \text{const}$ case is also shown. Two different configurations of the magnetic field are considered: $B_0 = 1 \text{ nG}$, $l_c = 1 \text{ Mpc}$ (left panel) and $B_0 = 100 \text{ nG}$, $l_c = 1 \text{ Mpc}$ (right panel).

We shall calculate below $\lambda(E, E_g^{\max})$, which according to Eq. (2) gives $r_{\max}^2/4$, where $r_{\max}(E)$ is the maximal distance from which protons with the observed energy E can arrive, as it follows from Eq. (1):

$$\lambda(E, E_g^{\max}) = \int_E^{E_g^{\max}} d\epsilon \frac{D(\epsilon)}{b(\epsilon)}. \quad (12)$$

In two extreme limits, at low energies and high energies, $\lambda(E, E_g^{\max})$ can be calculated analytically.

Let us start from the low-energy case $E \ll E_\beta$, when only adiabatic energy loss operates. Using $D(E) \propto E^\alpha$ we obtain from Eq. (12)

$$\lambda(E, E_g^{\max}) = \frac{D(E)}{\alpha H_0} \left[\left(\frac{E_g^{\max}}{E} \right)^\alpha - 1 \right]. \quad (13)$$

E_g^{\max} found from condition $\tau(E, E_g^{\max}) = t_0$ is $E_g^{\max} = E \exp(H_0 t_0)$, which results in

$$r_{\max}^{\text{diff}}(E) = 2 \left(\frac{D(E)}{\alpha H_0} \right)^{1/2} (e^{\alpha H_0 t_0} - 1)^{1/2}, \quad (14)$$

where according to the WMAP data (Spergel et al (2003)) $H_0 t_0 \approx 1$.

In the extreme high-energy regime $E \geq 3 \times 10^{20}$ eV $\tau_\pi^\infty = E(dE/dt)^{-1} \approx 4.1 \times 10^7$ yr does not depend on energy and from Eq. (12) we have

$$r_{\max}^{\text{diff}}(E) = \sqrt{2D_0\tau_\pi^\infty} \left(\frac{E_{\max}^{\text{acc}}}{E_c} \right). \quad (15)$$

Consider now the intermediate energies, when E approaches 1×10^{18} eV, but $E_g(E, t_0)$ remains less than $E_\pi \approx 4 \times 10^{19}$ eV, where photopion production starts. One obtains in the case $D(E) \propto E^\alpha$

$$r_{\max}^{\text{diff}}(E) \propto \sqrt{D_0\tau_{ee}} \left(\frac{E_g(E, t_0)}{E} \right)^{\alpha/2}, \quad (16)$$

where $\tau_{ee} \sim \beta_{e^+e^-}^{-1}$. In this case $r_{\max}^{\text{diff}}(E)$ grows fast with E due to the fast growth of $E_g(E, t_0)$ (see Fig. 2).

When E approaches $E_\beta \approx 2 \times 10^{18}$ eV, the value of r_{\max}^{diff} is determined by the energy interval between E_c and E_{\max}^{acc} , where $D(E) \propto E^2$. E_g^{\max} there grows by a jump to E_{\max}^{acc} , and r_{\max}^{diff} also grows by a jump to the high energy asymptotic value given by Eq. (15).

The accurate numerical calculations are displayed in Fig. 3 for two different magnetic field configurations (1 nG, 1 Mpc) and (100 nG, 1 Mpc), respectively.

In a diffusive regime of propagation there is an additional upper limit for a distance to a source, which we shall refer to as the rectilinear maximal distance $r_{\max}^{\text{rect}}(E)$. It is defined as

$$r_{\max}^{\text{rect}}(E) = \begin{cases} c\tau(E, E_g^{\max}) & \text{if } \tau < t_0, \\ ct_0 & \text{if } \tau > t_0. \end{cases} \quad (17)$$

At small E $r_{\max}^{\text{rect}}(E) \equiv c\tau(E, E_g^{\max}) = (c/H_0) \ln(E_g^{\max}/E)$ is larger than ct_0 and $r_{\max}^{\text{diff}}(E)$, as one can see from Fig. 3. At large E $r_{\max}^{\text{rect}}(E)$ is smaller than $r_{\max}^{\text{diff}}(E)$, and thus the rectilinear upper limit becomes restrictive.

The Syrovatsky solution (1) does not include automatically the restriction due to $r_{\max}^{\text{rect}}(E)$, because propagation time there varies from 0 to ∞ . The restriction (17) must be imposed in Eq. (1) additionally. This restriction is valid also in the case without magnetic field and numerically it is very close to the attenuation length $l_{\text{att}}(E) = E(dE/dl)^{-1}$, which describes the ordinary GZK cutoff.

Fig. 3 illustrates the antiGZK effect which we discuss here. While the energy-attenuation length $l_{\text{att}}(E) = E(dE/dl)^{-1}$ (or maximal rectilinear distance r_{\max}^{rect}) diminishes with energy E and has the sharp GZK steepening at $E \sim 5 \times 10^{19}$ eV, the diffusive maximum distance $r_{\max}^{\text{diff}}(E)$ increases with energy and has a sharp jump at energy $E_j \approx 2 \times 10^{18}$ eV. As we discussed above, this energy is determined entirely by energy losses and it does not depend on the diffusion parameters.

The growth of $r_{\max}^{\text{diff}}(E)$ depends on the diffusive regime, as it directly follows from Eq. (14).

4. Results and discussion

The maximum distance $r_{\max}(E)$ determines the number of sources which in principle can contribute to the observed diffuse flux $J_p(E)$: the flux from the sources at distances r larger than r_{\max} is suppressed as $\exp(-r^2/r_{\max}^2)$. But inside the sphere with radius r_{\max} the fluxes from the sources are suppressed by $\lambda(E, E_g)$, which is less than $\lambda(E, E_g^{\max})$ and by $E_g^{-\gamma_g}(E)$. By this reason, the jump in r_{\max} does not produce a jump in the flux at energy E_j . The situation is different at $E < 2 \times 10^{18}$ eV, where $r_{\max}(E)$ suppresses the diffuse flux, restricting the number of contributing sources.

In Figs 4,5,6 we present the calculated diffuse spectra using Eqs. (1) and (11), in the case of two configurations (B_0, l_c) and for different distances d between sources.

In our calculations the sources are located in the vertexes of a lattice, and summation is performed within the volume limited by $r_{\max}(E)$ as described in Section 3. In fact, only the rectilinear limit is introduced by hand, while $r_{\max}^{\text{diff}}(E)$ at lower energies appears automatically.

As was expected, the energy of the low-energy steepening E_s is nearly the same for all magnetic configurations and approximately coincides with the cross-over of adiabatic and pair-production energy losses E_β , and with the position of jump E_j . In accordance with $r_{\max}(E)$ given by Eq. (14), the flux below the low-energy cutoff is the largest for the Kolmogorov diffusion (or $D=\text{const}$ regime) and the lowest for $D(E) \propto E^2$ diffusion, with the Bohm diffusion between them.

In the calculations for a reasonable magnetic field configuration with $B_0 = 1$ nG and $l_c = 1$ Mpc, we have used a separation between sources $d = 30$ Mpc and $d = 50$ Mpc, which corresponds to a source space density 3.7×10^{-5} Mpc $^{-3}$ and 8.0×10^{-6} Mpc $^{-3}$, respectively. As was discussed in the Introduction, the small-angle clustering favors a density $n_s \sim (1 - 3) \times 10^{-5}$ Mpc $^{-3}$ with some uncertainties. In the case of strong magnetic field $B_0 = 100$ nG we have used a larger separation $d = 100$ Mpc to improve the agreement with observations.

In Figs 4 and 5 we show the spectra in the case $B_0 = 1$ nG and $l_c = 1$ Mpc. The critical energy where the diffusion changes its regime is $E_c \sim 1 \times 10^{18}$ eV, and the diffusion length at this energy is $l_{\text{diff}} \approx 1$ Mpc. The best fit to the observations is obtained for $\gamma_g = 2.7$. The energy of the steepening in both cases is $E_s \sim 1 \times 10^{18}$ eV. The source luminosities L_p , needed to provide the observed flux are very high, if one assumes a power-law generation

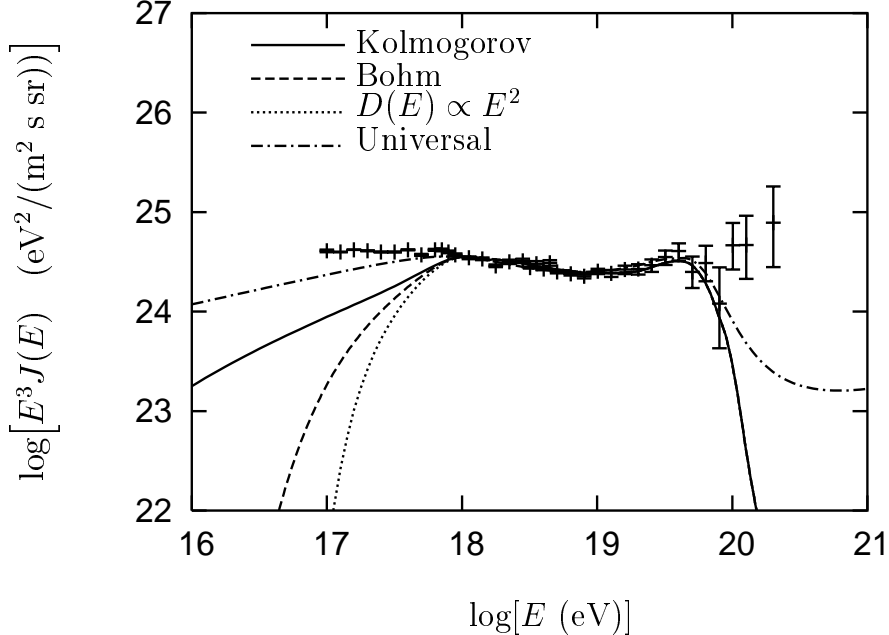


Fig. 4.— Energy spectrum in the case of $B_0 = 1 \text{ nG}$, $l_c = 1 \text{ Mpc}$ and for the diffusion regimes: Kolmogorov (continuous line), Bohm (dashed line) and $D(E) \propto E^2$ (dotted line). The separation between sources is $d = 50 \text{ Mpc}$ and the injection spectrum index is $\gamma_g = 2.7$ (see text). The AGASA-Akemo experimental data with the universal spectrum (dash-dotted line) are also reported.

spectrum from $E_{\min} \sim 1 \text{ GeV}$ up to $E_{\max}^{\text{acc}} = 1 \times 10^{22} \text{ eV}$. For $d = 50 \text{ Mpc}$ $L_p = 1.5 \times 10^{49} \text{ erg/s}$ and for $d = 30 \text{ Mpc}$ $L_p = 3.0 \times 10^{48} \text{ erg/s}$. To reduce these luminosities one can assume that the acceleration mechanism operates starting from some larger E_{\min} . Then the required luminosity is reduced by a factor $E_{\text{GeV}}^{-(\gamma_g-2)}$, which is 1.3×10^{-5} for $E_{\min} = 1 \times 10^8 \text{ GeV}$, and 2.5×10^{-6} for $E_{\min} = 1 \times 10^9 \text{ GeV}$. Another possible assumption is the standard spectrum $\propto 1/E^2$ at $E < E_{\min}$ as Berezinsky et al (2002b) have assumed.

Figs 4 and 5 show that the dip seen in the universal spectrum as a signature of the interaction with CMB (Berezinsky et al 2002a) survives in the case of propagation in magnetic field with configuration $(1 \text{ nG}, 1 \text{ Mpc})$. As will be shown below the same is true for weaker and stronger magnetic fields.

The case of a strong magnetic field $(B_0, l_c) = (100 \text{ nG}, 1 \text{ Mpc})$ is shown in Fig. 6. This is a very attractive case: the good agreement with the data is reached using the standard generation spectrum $\propto 1/E^2$ and $d = 100 \text{ Mpc}$. The required luminosity is reasonable, $L_p = 3 \times 10^{45} \text{ erg/s}$ for $E_{\min} \sim 1 \text{ GeV}$ and $E_{\max} = 1 \times 10^{22} \text{ eV}$. The diffusion coefficient used

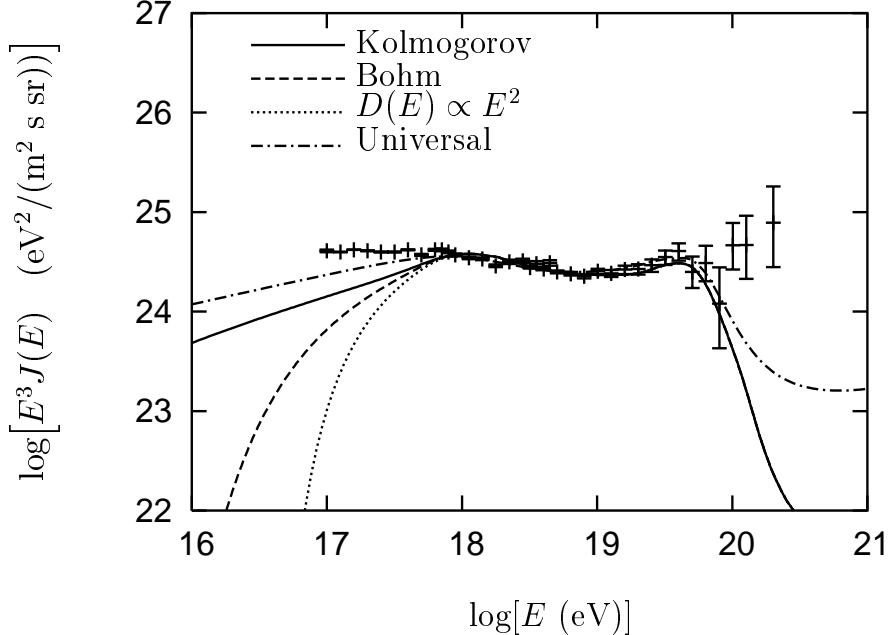


Fig. 5.— The same as in Fig. 4, but for smaller separation between sources $d = 30$ Mpc. Notice the better conversion to the universal spectrum than in the case with $d = 50$ Mpc, shown in Fig. 4.

in this case is $D \approx \text{const}$ at $E \lesssim E_c$ (the best fit in Fig. 6 is obtained for $D(E) \propto E^{0.02}$). Unfortunately, the required magnetic field is much higher than that obtained in the MHD simulations by Dolag et al. (2004) and Sigl et al. (2004), though it does not contradict the existing observational upper limits.

Let us now come over to the case of very weak magnetic field $B_0 \sim 0.1$ nG, favored by MHD simulations by Dolag et al (2004). In this case $E_c \approx 1 \times 10^{17} (l_c/1 \text{ Mpc})$ eV and $l_{\text{diff}}(E) \approx 100 E_{18}^2 (1 \text{ Mpc}/l_c)$ Mpc. Therefore, for $l_c \lesssim 1$ Mpc and $E \gtrsim 3 \times 10^{18}$ eV the protons propagate quasi-rectilinearly in the universe. In this case the distance between sources d is less than the propagation lengths $l_{\text{diff}}(E)$ and $l_{\text{att}}(E)$, and the spectrum at least at energies $(1 - 40) \times 10^{18}$ eV must be universal.

A note of warning should be made about the validity of the Syrovatsky solution at $E < 1 \times 10^{19}$ eV. This solution is expected to work not perfectly well at these energies, because it is valid only in the case when the energy losses $b(E)$ and diffusion coefficient $D(E)$ are time-independent¹. For the above-mentioned energies this is not the case, because

¹One should be careful with inserting ad hoc time-dependent quantities in the Syrovatsky solution (1),

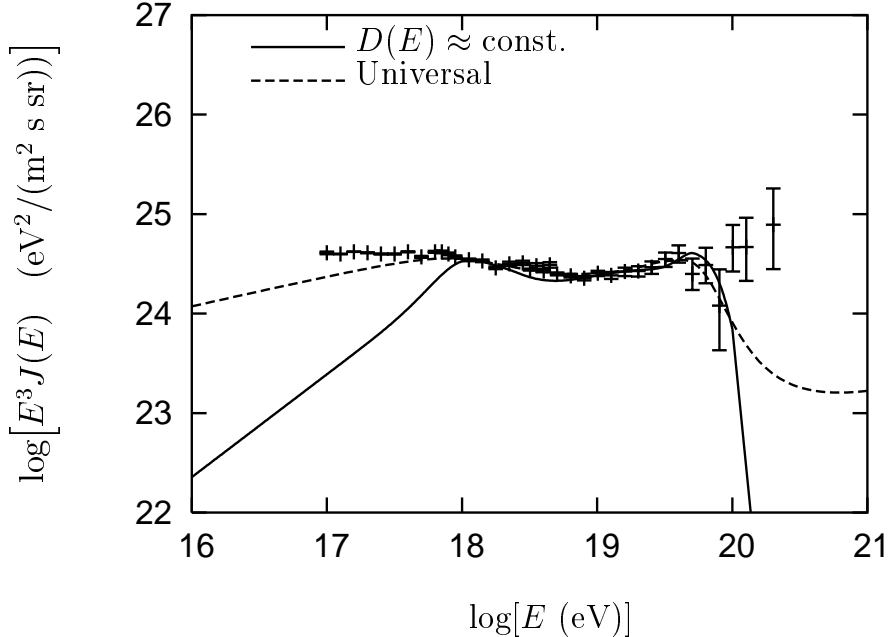


Fig. 6.— Differential spectrum in the case of $B_0 = 100 \text{ nG}$, $l_c = 1 \text{ Mpc}$ and for the diffusion regime with $D(E) \simeq \text{const.}$ The separation between sources is $d = 100 \text{ Mpc}$ and the injection spectrum is the standard one ($\gamma_g = 2$). The AGASA-Akeno experimental data with the universal spectrum (dashed line) are also shown. The sharp cutoff in the energy spectrum at the highest energies is due to large distances to the nearby sources $r \sim d \sim 100 \text{ Mpc}$.

during the time of propagation the temperature of the CMB radiation changes appreciably, and hence the energy losses too². The diffusion equation itself should be also modified as $t \rightarrow t_0$ by the cosmological relations between time and distance. However, the approximate agreement, which we obtained (to be discussed somewhere else) between the Syrovatsky solution in quasi-rectilinear regime and the exact rectilinear propagation demonstrates the approximate validity of this solution at the discussed energies.

Another argument in favor of the Syrovatsky solution as a reasonable approximation at the discussed energies $E \lesssim 1 \times 10^{19} \text{ eV}$ is the convergence to the universal spectrum (compare Fig. 4 and Fig. 5 for $d = 50 \text{ Mpc}$ and $d = 30 \text{ Mpc}$, respectively). The universal spectrum is

because in this case it ceases to be a solution of the corresponding diffusion equation. For example, it is forbidden to introduce the cosmological scaling factor $a(t)$, because it results in time dependent energy losses $b(E, t)$, or considering λ in Eq. (1) as function of E, E_g and t .

²In our previous paper, Aloisio and Berezinsky (2004), we deliberately limited ourselves to higher energies.

calculated in the case of time-dependent CMB temperature and for an expanding universe. The Syrovatsky solution converges to this spectrum with accuracy better than 15% when $d \rightarrow 3 - 5$ Mpc (to be discussed somewhere else).

Following the papers by Berezinsky et al (2004) and Lemoine (2004), we shall now discuss shortly the transition from galactic to extragalactic cosmic rays. The remarkable feature of the diffusive spectra is the low-energy steepening at the fixed energy $E_s \sim 1 \times 10^{18}$ eV, which provide the transition from extragalactic to galactic CR. This energy coincides approximately with the position of the second knee E_{sk} and gives a non-trivial explanation of its value as $E_{\text{sk}} \sim E_\beta$.

Like in the above-mentioned works we shall assume that at $E \gtrsim 1 \times 10^{17}$ eV the galactic spectrum is dominated by iron nuclei and calculate their flux by subtracting the calculated flux of extragalactic protons from all-particle Akeno spectrum. For these calculations we shall fix the spectrum with magnetic configuration (1 nG, 1 Mpc), the Bohm diffusion at $E < E_c$ and a separation between sources on the lattice $d = 30$ Mpc (see Fig. 5). The calculated spectrum of galactic iron is shown in Fig. 7 by the dashed curve. The fraction of iron-nuclei in the total flux is shown in Table 1 as a function of energy. This prediction should be taken with caution because of the model-dependent calculations (assumption of the Bohm diffusion) and uncertainties involved in the Syrovatsky solution. However, it is interesting to note that the iron-nuclei spectrum in Fig. 7 practically coincides with the spectrum calculated by Berezinsky et al. (2004) for the model with the generation spectrum steepening. The iron-nuclei spectra in both cases are well described by the Hall diffusion (Ptuskin et al. (1993)) in the galactic magnetic field at energies above the knee.

We shall compare now our results with those obtained by Lemoine (2004), who also found the low-energy steepening of the spectrum due to diffusion. Lemoine has limited his calculations to the case $B_0 \sqrt{l_c} \sim 2 \times 10^{-10}$ GMpc $^{1/2}$, while we demonstrated that this phenomenon is valid for much wider range of parameters, for example our configuration (100 nG, 1 Mpc) corresponds to the Lemoine parameter two order of magnitude larger. We considered here a more realistic basic scale $l_c \sim 1$ Mpc and the various regimes of diffusion, while Lemoine limited himself to the $D(E) \propto E^2$ regime only. We have also obtained the important result that the energy of the steepening is the same, $E_s \sim 1 \times 10^{18}$ eV, for all diffusion regimes and distances between the sources, and that universality is determined almost entirely by the proton energy losses. We discussed the diffusive anti-GZK effect, which we consider as the most interesting observation of this work³.

³Our work has been performed independently from the paper by Lemoine (2004) and much earlier. We discussed our results with Pasquale Blasi in September 2004. The delay with the publication was partly

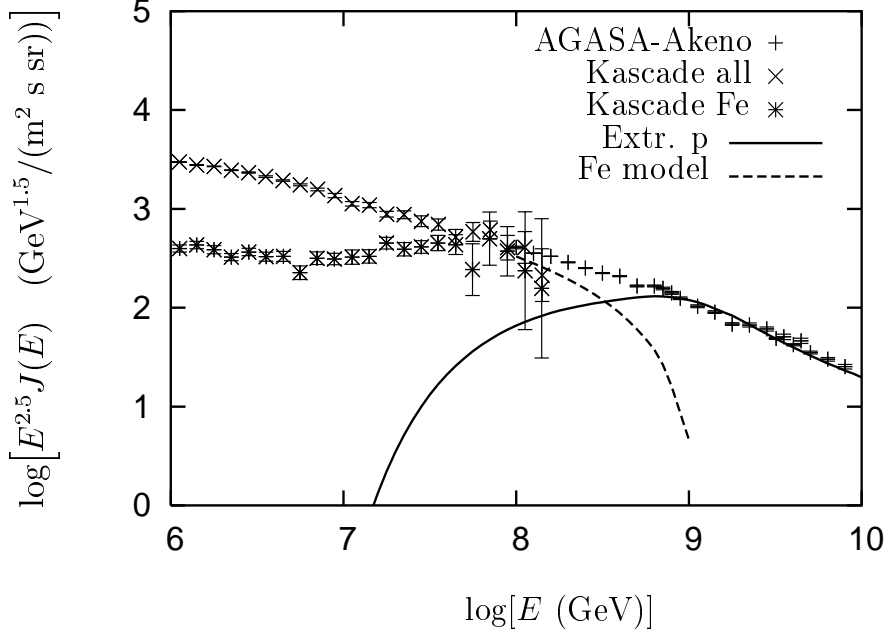


Fig. 7.— The galactic iron-nuclei spectrum computed by subtracting the extragalactic proton spectrum from the Akeno-AGASA data. The extragalactic proton spectrum is taken for the case $B_0 = 1$ nG, $l_c = 1$ Mpc, $d = 30$ Mpc, $\gamma_g = 2.7$ with the Bohm diffusion at $E < E_c$.

5. Conclusions

We have analyzed in this paper the anti-GZK effect in the diffusive propagation of ultra high energy protons. This effect consists in an increase of the maximum distance $r_{\max}(E)$, from which ultra high energy protons can reach an observer, with an increasing of the energy E . This increase is terminated by a jump, which is located at energy $E_j \approx 2 \times 10^{18}$ eV. The position of the jump is determined exclusively by energy losses (transition from adiabatic to pair-production energy losses) and it is independent of the diffusion parameters. The position of the jump practically coincides with the position of the aforementioned transition and gives approximately the position of the second knee observed in the cosmic ray spectrum (see below).

The observational consequences of the antiGZK effect is the low-energy “cutoff” of the diffuse spectrum, which is in fact a steepening in the spectrum, as the GZK cutoff is. The steepening energy E_s coincides approximately with the position of the jump, $E_s \sim E_j$, and it is also practically independent of the diffusion parameters, i.e. of the basic scale of

connected with our attempts to overcome the problems of the Syrovatsky solution.

E (eV)	10^{17}	2×10^{17}	5×10^{17}	7×10^{17}	10^{18}
$J_{Fe}/(J_p + J_{Fe})$	0.83	0.66	0.32	0.17	0.04

Table 1: Fraction of iron-nuclei in the total flux as function of the energy.

magnetic field coherence l_c and of the magnetic field B_0 on this scale. However, the shape of the steepening is determined by the diffusion regime: it is most steep in case $D(E) \propto E^2$ diffusion, most flat in case of the Kolmogorov diffusion, with the Bohm diffusion between them.

In our calculations we have used the Syrovatsky solution to the diffusion equation, combined with the rectilinear propagation at the appropriate distances. The sources are located in the vertexes of a lattice with a spacing scale d (the source separation). We have used mostly $d = 30$ Mpc and $d = 50$ Mpc, which correspond to a space density of the sources 3.7×10^{-5} Mpc $^{-3}$ and 8.0×10^{-6} Mpc $^{-3}$, respectively. The observed small-angle clustering favors the density $n_s \sim (1 - 3) \times 10^{-5}$ Mpc $^{-3}$. The diffusion coefficient $D(E)$ is calculated for a random magnetic field with the basic scale l_c and the coherent magnetic field on this scale B_0 . Using this approach we have calculated the diffusive spectra for various magnetic configurations (B_0, l_c) and source separations d .

Physically the most reasonable case corresponds to a magnetic field configuration (1 nG, 1 Mpc) with a source separation $d = 30$ Mpc and $d = 50$ Mpc. The calculated spectra are shown in Figs 4 and 5 in comparison with Akeno-AGASA data. For a power-law generation spectrum with $\gamma_g = 2.7$ the agreement is good, but needs too high luminosity of the sources L_p , if the power-law spectrum starts with low energy $E_{\min} \sim 1$ GeV. This problem can be ameliorated assuming higher values of E_{\min} .

The calculated diffusive spectra in the energy interval $(1 - 80) \times 10^{18}$ eV agree perfectly well with the universal spectrum and experimental data, showing the presence of the dip caused by e^+e^- production.

An interesting case is given by the diffusion in strong magnetic field with basic configuration (100 nG, 1 Mpc) and source separation $d = 100$ Mpc. In this case (Fig 6) the best fit of the spectrum is obtained for the standard acceleration spectrum $Q(E) \propto 1/E^2$ and $E_{\min} \sim 1$ GeV. The required luminosity is $L_p = 3 \times 10^{45}$ erg/s. Up to energy $E \sim 1 \times 10^{20}$ eV the predicted spectrum agrees with data of both detectors, AGASA and HiRes. The sharp cutoff at $E \sim 1 \times 10^{20}$ eV is produced due to large distances $r \sim d$ to the nearby sources. For the explanation of the AGASA excess at $E \gtrsim 1 \times 10^{20}$ eV a new component of ultra high energy cosmic rays (e.g. from superheavy dark matter, see Aloisio et al 2004) is needed.

At energies $E < E_s$, where l_{diff} becomes much smaller than d , the diffusive spectrum exhibits a steepening in contrast to the universal spectrum (see Figs 4 - 6).

The steepening of the spectrum at $E_s \sim 1 \times 10^{18}$ eV provides a natural transition from galactic to extragalactic cosmic rays. This energy coincides with the second knee observed in cosmic rays spectra by most of the detectors. While the energy of the transition E_s (and thus position of the second knee) is predicted in a model independent way, the shape of the proton spectrum below 1×10^{18} eV and the fraction of galactic iron nuclei are model dependent: they differ for various diffusion regimes.

Acknowledgments

We are grateful to Pasquale Blasi for useful discussion. We thank the transnational access to research infrastructures (TARI) program through the LNGS TARI grant contract HPRI-CT-2001-00149.

REFERENCES

R. Aloisio and V.S. Berezinsky, Ap.J. **612**, 900 (2004).

R. Aloisio, V.S. Berezinsky and M. Kachelriess, Phys. Rev. D **69**, 094023 (2004).

V.S. Berezinsky, V.A. Dogiel and S.I. Grigorieva, A&A **232**, 582 (1990a).

V.S. Berezinsky, A.Z. Gazizov and S.I. Grigorieva, (2002a) hep-ph/0204357.

V.S. Berezinsky, A.Z. Gazizov, and S.I. Grigorieva, (2002b) astro-ph/0210095.

V.S. Berezinsky, A.Z. Gazizov and S.I. Grigorieva, (2003) hep-ph/0302483, Proc. of Int. Workshop “Extremely High Energy Cosmic Rays” (eds M.Teshima and T.Ebisuzaki), Universal Academy Press, Tokyo 63, 2003.

V.S. Berezinsky, S.I. Grigorieva and B.I. Hnatyk, Astrop. Phys. **21**, 617 (2004).

P. Blasi and D. De Marco, Astrop. Phys. **20**, 559 (2004).

P. Blasi, S. Burles, A.V. Olinto, Ap.J. **514**, 79 (1999a).

P. Blasi and A.V. Olinto, Phys. Rev. D**59** 023001 (1999b).

C.L. Carilli and G.B. Taylor, Annual Rev. Astr. Astroph., **40**, 319 (2002).

F. Casse, M. Lemoine and G. Pelletier, Phys. Rev. **D65** 023002 (2002).

O. Deligny, A. Letessier-Selvon and E. Parizot, astro-ph/0303624.

K. Dolag, D. Grasso, V. Springel and I. Tkachev, astro-ph/0310902.

S.L. Dubovsky, P.G. Tinyakov and I. Tkachev, Phys. Rev. Lett. **85**, 1154 (2000).

Z. Fodor and S.D. Katz, Phys. Rev. **D63**, 023002 (2001).

M. Giller, J. Wdowczyk and A.W. Wolfendale, J.Phys. G **6** 1561 (1980).

A.V. Glushkov and M.I. Pravdin, Astronomy Lett. **27**, 493 (2001).

K. Greisen, Phys. Rev. Lett. **16**, 748 (1966).

D. Harari, S. Mollerach and E. Roulet, JHEP 0207 006 (2002).

N. Hayashida et al. (AGASA collaboration), Phys. Rev. Lett. **77** 1000 (1996).

N. Hayashida et al. (AGASA collaboration), Ap.J., **522**, 225 (1999).

M. Kachelrieß and D. Semikoz, astro-ph/0405258.

P.P. Kronberg, Rep. Progr. Phys. **57**, 325 (1994).

M. Lemoine, G. Sigl and P. Biermann, astro-ph/9903124.

M. Lemoine, astro-ph/0411173.

V.S. Ptuskin et al., Astron.Astroph. **268**, 726 (1993).

D. Ryu, H. Kang and P. Biermann, Astron. Astroph., **335**, 19 (1998).

G. Sigl, M. Lemoine and P. Biermann, Astrop. Phys. **10** 141 (1999).

G. Sigl, F. Miniati and T.A. Enßlin, Phys. Rev. **D68** 043002 (2003).

G. Sigl, F. Miniati and T.A. Enßlin, astro-ph/0401084.

D.N. Spergel et al (WMAP collaboration), Astrophys. J. Suppl. **148** (2003) 175.

T. Stanev et al, Phys. Rev. **D 62** 093005 (2000).

S.I. Syrovatskii, Sov. Astron. **3** 22 (1959).

P.G. Tinyakov and I. Tkachev, JETP Lett., **74** 445 (2001).

Y. Uchiori et al, Asrop. Phys. **13**, 157 (2000).

J.P. Vallee, Fund. Cosm. Phys. **19**, 1 (1997).

J. Wdowczyk and A.W. Wolfendale, Nature, **281**, 356 (1979).

H. Yoshiguchi, S. Nagataki, S. Tsubaki and K. Sato, Astrophys.J. 586 (2003) 1211-1231.

G.T. Zatsepin and V.A. Kuzmin, JETP Lett. **4**, 78 (1966).